Geodinamica Acta, 2016
Vol. 28, No. 4, 254–272, http://dx.doi.org/10.1080/09853111.2016.1171111

Taylor & Francis
Taylor & Francis Group

Palaeoseismology of the Havran-Balıkesir Fault Zone: evidence for past earthquakes in the strike-slip-dominated contractional deformation along the southern branches of the North Anatolian fault in northwest Turkey

Hasan Sözbilir[a,b]*, Çağlar Özkaymak[c,d], Bora Uzel[a], Ökmen Sümer[a], Semih Eski[b] and Çiğdem Tepe[a]

[a]*Department of Geological Engineering, Dokuz Eylül University, İzmir TR-35160, Turkey;* [b]*Earthquake Research and Implementation Center of Dokuz Eylül University, İzmir TR-35160, Turkey;* [c]*Department of Geological Engineering, Afyon Kocatepe University, Afyon TR-03200, Turkey;* [d]*Earthquake Research and Implementation Center of Afyon Kocatepe University, Afyon TR-03200, Turkey*

(*Received 22 January 2016; accepted 23 March 2016*)

The Havran-Balıkesir Fault Zone (HBFZ) is one of the major active structures of the Southern Marmara Region, which has been shaped by the southern branch of North Anatolian fault since the Pliocene. HBFZ is a 10–12 km wide, 120 km long, right-lateral strike-slip fault zone that consists of two ENE-striking main faults, namely, the Havran-Balya and Balıkesir faults. The 90-km-long Havran-Balya fault exhibits right-stepping en echelon geometry and is made up of (1) Havran, (2) Osmanlar, (3) Turplu and (4) Ovacık fault segments. On the eastern part, the 70-km-long Balıkesir fault is divided into two fault segments; (1) Gökçeyazı and (2) Kepsut. We estimated the long-term slip rate between 3.59 and 3.78 mm/yr using river offset. The Kepsut, Gökçeyazı and Ovacık fault segments are capable of generating an earthquake with a moment magnitude of up to 7.2. Detailed palaeoseismological studies show that the HBFZ is responsible for some surface faulting earthquakes with an average recurrence interval of 1000–2000 years during the late Holocene. Considering the fact that there was no evidence of a surface-ruptured earthquake for 2000 years, it can be stated that there is a seismic gap on the Gökçeyazı fault segment.

Keywords: North Anatolian fault zone; North-west Turkey; Havran-Balıkesir Fault Zone; palaeoseismology; slip rate

1. Introduction

The left-lateral East Anatolian fault and the right-lateral North Anatolian fault (NAF) are the major sources of the large earthquakes in Turkey, and together they cause westward motion of the Anatolian block in response to the collision of Arabia with Eurasia and subduction roll-back along the Aegean trench (Figure 1(b)) (Bozkurt, 2001; McClusky, Reilinger, Mahmoud, Ben Sari, & Tealeb, 2003; McKenzie, 1972; Şengör, 1979). The NAF, which is one of the most active seismogenic zones in the world, separates the Eurasian and Anatolian blocks and is responsible for the westward tectonic escape of the Anatolian Plate since the Pliocene (Bozkurt, 2001; Ketin, 1957; McKenzie, 1972; Şengör, 1979; Şengör, Görür, & Şaroğlu, 1985; Şengör et al., 2005). The fault trace of the E–W-trending NAF is divided into two branches around Düzce city towards the north-west of Turkey (Özalp, Emre, & Doğan, 2013; Şengör & Barka, 1992). The northern branch, which generated İzmit (M_w: 7.4) and Düzce (M_w: 7.2) earthquakes in 1999 (Taymaz, Yılmaz, & Dilek, 2007), passes through the Sapanca-Kocaeli corridor and enters into the Marmara Sea. The southern branch, which generated the Yenice (M_w: 7.2) (McKenzie, 1972) and Manyas (M_S: 6.8) (Taymaz, Jackson, & Mc Kenzie, 1991) earthquakes in 1953 and 1964, respectively, is represented by many parallel/subparallel dextral strike slip faults that lie between the İznik and Aegean Sea along the Southern Marmara Region (SMR). One of the seismically active structures in SMR is known as the Havran-Balıkesir Fault Zone (HBFZ) (Emre, Doğan, & Özalp, 2011). It extends about 120 km between the Havran to the west and Kepsut to the east and bounds the southern margin of the SMR (Figure 1(c)). Global Positioning System (GPS) measurements indicate that the slip rate on the North Anatolian fault is ~20–25 mm/yr in the Marmara region (McClusky et al., 2003; Reilinger et al., 2006). In this part, the rate of motion between the Anatolian block and Eurasian blocks are shared by these two branches. The short-term slip rate on the southern branches is attributed to about 5–7 mm/yr, while the slip rate of northern branch of the NAF is about 17 mm/yr (Armijo, Meyer, Hubert, & Barka, 1999; Klinger et al., 2003). Besides this, Meade et al. (2002) suggest that the approximate slip rate is between 6.8 ± 2.3 and 3.6 ± 2.3 mm/yr for the southern branch of NAF, according to geodetic studies. Although the fact that northern branch of the NAFZ is more active than the southern branch (Barka, 1997; Klinger et al., 2003; Kürçer et al., 2008; McClusky et al., 2003; Rockwell, Barka, Dawson, Akyüz, & Thorup, 2001), seismologic records and some palaeoseismological studies carried out in the SMR reveal that the

*Corresponding author. Email: hasan.sozbilir@deu.edu.tr

© 2016 Informa UK Limited, trading as Taylor & Francis Group

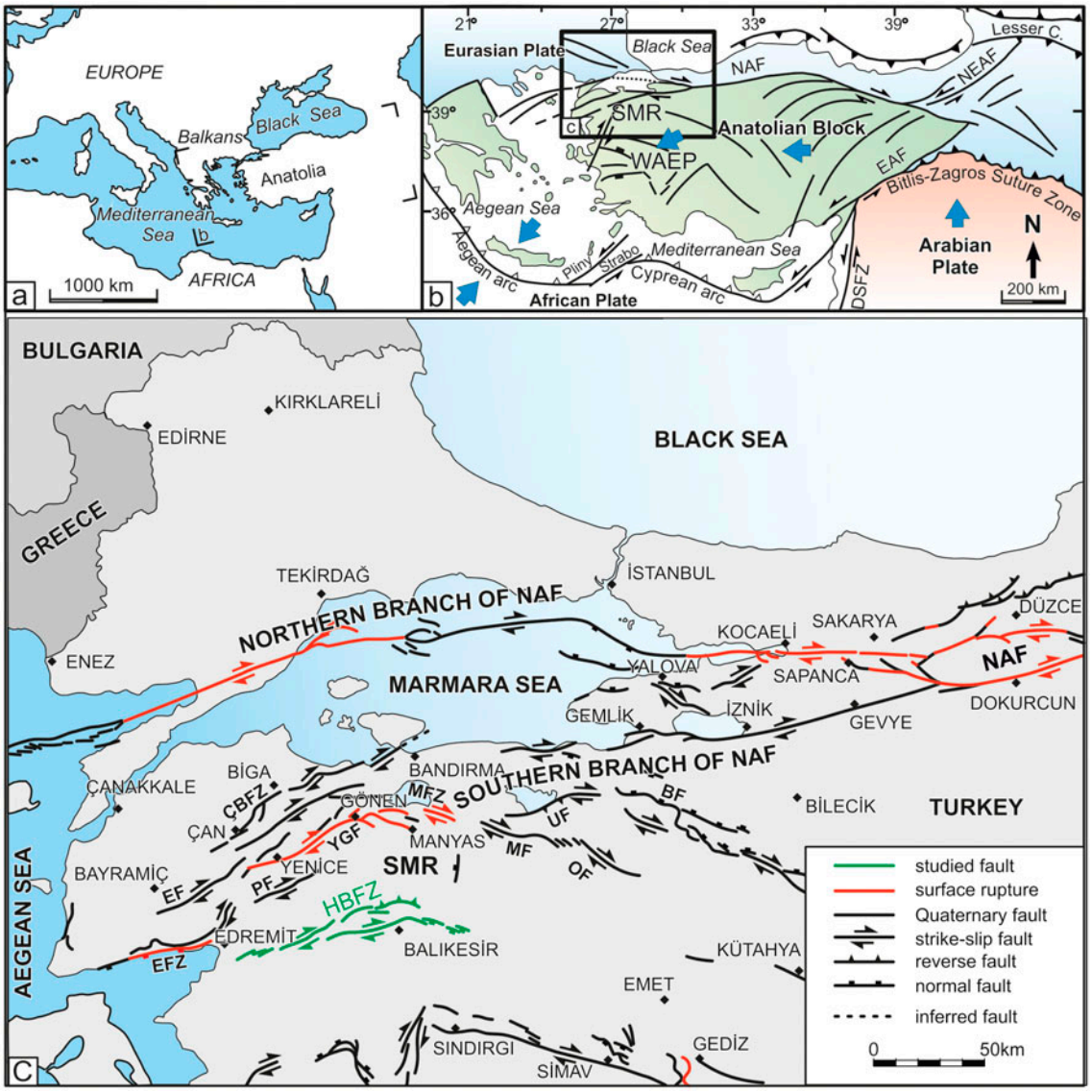


Figure 1. (a) Location of the Anatolia in global scale, (b) Tectonic outline of eastern Mediterranean area (compiled from Kaymakcı, 2006; Özkaymak, 2015). Abbreviations: SMR, Southern Marmara Region; WAEP, West Anatolian Extensional Provinces; DSFZ, Dead Sea Fault Zone; EAF, East Anatolian Fault; NAF, North Anatolian Fault; NEAF, Northeast Anatolian Fault. (c) Simplifed active fault map of Northwest Anatolia (modified from Emre & Doğan, 2010; Emre et al., 2013). Abbreviations: BF, Bursa Fault; UF, Ulubat Fault; MF, Mustafakemalpaşa Fault; OF, Orhangazi Fault; MFZ, Manyas Fault Zone; YGF, Yenice–Gönen Fault; ÇBFZ, Çan-Biga Fault Zone; EF, Evciler Fault; PF, Pazarköy Fault; EFZ, Edremit Fault Zone and the HBFZ, Havran-Balıkesir Fault Zone.

southern branch of the North Anatolian fault also has a potential to generate large earthquakes (Belindir, 2008; Kürçer et al., 2008; Özalp et al., 2013; Tan, Tapırdamaz, & Yörük, 2008; Yoshioka & Kuşcu, 1994). Therefore, the palaeoseismological record from such segments is important to hazard assessments. Nevertheless, paleoseismic data from the southern branch of NAF are still scarce. This paper outlines the segment characteristics and geomorphic analysis of HBFZ using field study techniques such as geological mapping; then, it first considers and interprets data from the trench-based palaeoseismological investigations: direct dating of past faulting events together with estimates of long-term slip-rates and recurrence intervals.

2. Seismotectonic setting

The active tectonics of the SMR are governed dominantly by the southern branch of NAF. From north to south, the Çan-Biga Fault Zone (ÇBFZ), Manyas Fault Zone (MFZ), Yenice–Gönen Fault (YGF), Evciler Fault (EF), Pazarköy Fault (PF), Edremit Fault Zone (EFZ) and the HBFZ are the major right-lateral strike slip faults in the southwestern margin of the SMR (Figure 1(c)). Large historical earthquakes, which are summarised in Table 1, were reported in the SMR between 160 AD and 1899 AD (Ambraseys, 2002; Ambraseys & Finkel, 1995; Ambraseys & Jackson, 1998; Ergin, Güçlü, & Uz, 1967; Papazachos & Papazachou, 2003; Shebalin, Karnik, & Hadzievski, 1974; Soysal, Sipahioğlu, Kolçak, &

Table 1. List of recorded historical earthquakes in the Balıkesir region.

No	Date	Coordinate lat. (N)–long. (E)	Locality affected	I	M	Reference
1	160	40.00–27.50	Yenice, Gönen, Biga	–	M_S: 7.1	1
2	253	39.10–27.15	Bergama	IX	–	2, 3, 4
3	17.07.1296	39.10–27.45	Bergama, Dikili, Soma, Balıkesir	VII	M_w: 6.9	2, 4, 5
4	21.09.1577	39.70/27.70	Balıkesir	?	–	6
5	10.09.1688	39.65/27.80	Balıkesir	VIII-IX	M_w: 6.6	6, 7, 8
6	08.02.1826	39.50/28.00	Balıkesir	VIII	–	2, 3
7	10.08.1870	39.90/27.30	Balıkesir and Çanakkale	VII	M_w: 5.8	2, 3, 4
8	?.12.1897	39.60/27.90	Balıkesir	VIII	–	2, 3, 4, 8
9	28.02.1898	39.60/27.90	Balıkesir	VIII	M_w: 6.9	3, 4

Notes: I – intensity and M – magnitude. M_w values are taken from Stucchi et al. (2013).
Source: References: (1) Ambraseys (2002); (2) Ergin et al. (1967); (3) Soysal et al. (1981); (4) Tan et al. (2008); (5) Ambraseys and Jackson (1998); (6) Ambraseys and Finkel (1995); (7) Papazachos and Papazachou (2003); (8) Shebalin et al. (1974).

Altınok, 1981). According to the historical records, two destructive earthquakes occurred near Yenice, Gönen, Biga and Bergama in 160 (M_S: 7.1) and 253 (I:IX) AD in centre of the SMR, but there is no detailed information about these events (Ambraseys, 2002; Ergin et al., 1967; Soysal et al., 1981). Ambraseys and Jackson (1998) refer to an earthquake in Balıkesir and surrounding areas in 1296 (M_w: 6.9, Table 1). According to the Ambraseys and Finkel (1995), Balıkesir city was shaken by an earthquake in 1577 that caused serious damage to the Balıkesir city area and caused at least 40 deaths (Figure 2 and Table 1). The 10 September 1688 earthquake shook İstanbul, Limnos, lesbos, Chios and İzmir in northwestern Anatolia. The location of this earthquake is given as the city centre of Balıkesir (Karesi) (Ambraseys & Finkel, 1995). Its magnitude was $M_w = 6.6$ (Stucchi et al., 2013), and its intensity was VIII–IX (Papazachos & Papazachou, 2003). After medium-scale earthquakes in 1826 and 1870, the last historical and destructive earthquakes with an intensity of VIII, which damaged the city of Balıkesir, occurred on 1897 and 1898 ($M_w = 6.9$) (Ergin et al., 1967; Shebalin et al., 1974; Soysal et al., 1981; Stucchi et al., 2013). The main shock affected Balıkesir, Kepsut and Bigadiç. According to Emre, Doğan, and Yıldırım (2012), surface rupturing associated with the 1897 or 1898 Balıkesir earthquakes probably occurred along the eastern segment of the HBFZ (Figure 2 and Table 1).

One of the strongest earthquakes during the instrumental period in the SMR occurred on the EFZ. The 1944 Edremit earthquake (M_w: 6.8) took place on the northern coast of the Edremit gulf and was responsible for the 37 km-long surface rupture (Altınok, Alpar, Yaltırak, Pınar, & Özer, 2012; Ambraseys, 1988; Ambraseys & Jackson, 1998; Yaltırak, 2006; Zimmermann, 1945). The focal mechanism of an earthquake indicates predominantly normal faulting with the tension axis trending approximately north–south (Taymaz et al., 1991). In 18 March 1953, a destructive earthquake (M_w: 7.2) occurred on YGF and caused a 50–70 km-long dextral surface rupture with an average 1.5 m of right lateral offset (Herece, 1990; Kürçer et al., 2008). The focal mechanism solution (FMS) of the earthquake indicates the existence of an almost pure strike-slip faulting (McKenzie, 1972). Studies estimating the recurrence interval of the southern branch of the NAF are limited and inadequate. According to the palaeoseismologic studies in the central part of the SMR that were performed along the YGF, estimates of the recurrence interval were between 660 ± 160 and 420 ± 170 years (Belindir, 2008; Kürçer et al., 2008) for surface faulting earthquakes, and the slip-rate was estimated as 6.3 mm/yr (Kürçer et al., 2008). Recent palaeoseismologic studies carried out on the Gemlik and İznik-Mekece faults in the eastern part of the SMR indicates that the recurrence intervals are 595 and 1700–2200 years, respectively (Özalp et al., 2013; Yoshioka & Kuşcu, 1994). In the SMR, the last destructive earthquake (M_S: 6.8) was recorded in 1964, which produced E–W-trending right-lateral strike-slip surface deformations on MFZ (Ketin, 1966). Although many destructive earthquakes were recorded in the Balıkesir vicinity during the historical period, there is no evidence of a surface rupture event during the instrumental period along the HBFZ. However, medium-scale earthquakes with magnitudes between 4.0 and 5.0 have frequently occurred along the zone (Figure 2), indicating that the HBFZ has a potential for earthquakes. The FMS of one of them, i.e. the 29 September 2007 Balıkesir earthquake, suggest a NE–SW contraction in the centre of the HBFZ (Figure 2) (Kalafat et al., 2009).

3. The HBFZ: fault geometry and segment characteristics

HBFZ is a major active structure lying between Eyüpbükü to the east and Küçükdere to the west and marked morphologically by the deep linear valleys and shutter ridges that forms the southern margin of the SMR. It can best be described as a transition zone between the strike-slip-dominated NAF (Armijo et al., 1999; Barka, 1992; Gürer, Kaymakçı, Çakır, & Özburan, 2003) and extension-dominated Aegean region (Özkaymak & Sözbilir, 2012; Özkaymak, Sözbilir, & Uzel, 2013; Sözbilir, 2001; Sözbilir, Sarı, Uzel, Sümer, & Akkiraz, 2011; Sümer, İnci, & Sözbilir, 2013; Uzel,

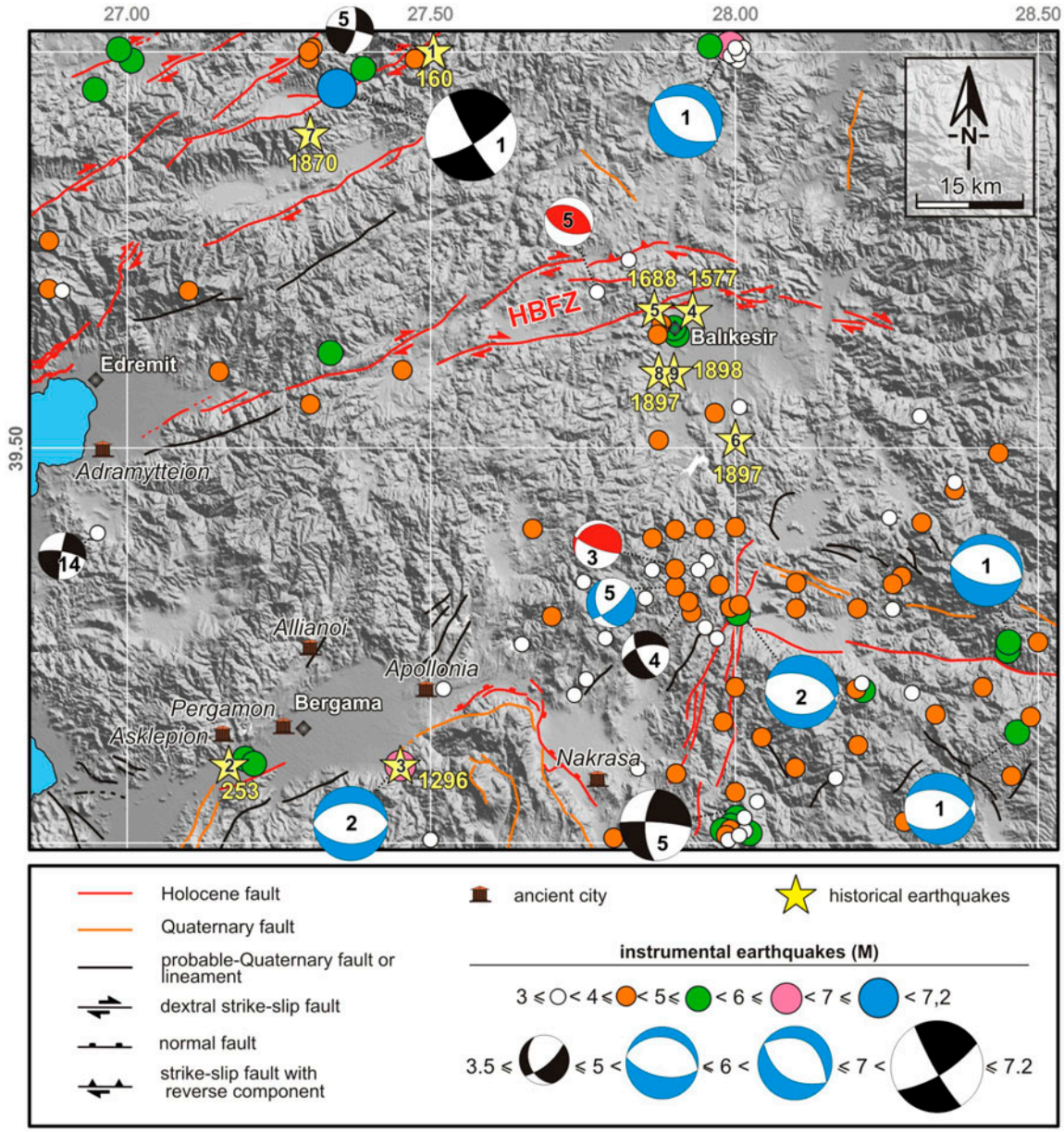


Figure 2. Seismotectonic map of the Balıkesir and surrounding area, showing the epicentres of both instrumental and historical earthquakes.
Notes: For the numbering of the historical earthquakes, see Table 1. Focal mechanism solution (FMS) of earthquakes are taken from (1) McKenzie (1972); (2) Euro-Med Seismological Centre (EMSC); (3) Kalafat (1998); (4) Tan and Taymaz (2004); (5) Kalafat et al. (2009).

Sözbilir, Özkaymak, Kaymakcı, & Langereis, 2013). HBFZ cuts and deforms five geologic units outcropping around Balıkesir: metamorphic rocks of the late Permian–Triassic Karakaya Complex, ophiolitic melange and flysch-type depositions of late Cretaceous-Palaeocene İzmir-Ankara Zone, Oligo-Miocene magmatic and volcano sedimentary rocks, earl-late Miocene continental clastics and Quaternary alluvial/colluvial/fluvial deposits (Figure 3). The Quaternary sediments are generally deposited along the linear valleys and also small-scale restraining and releasing bends of HBFZ. Emre et al. (2011) suggest that the fault zone consists of two E–W-striking faults, namely, Havran-Balya and Balıkesir faults from west to east (Figure 3). The ~90-km-long Havran-Balya fault exhibits right-stepping en echelon geometry and is made up of (1) Havran (HS), (2) Osmanlar (OS), (3) Turplu (TS) and (4) Ovacık (OvS) fault segments. On the eastern part, the 70-km-long Balıkesir fault is divided into two segments based on the geomorphological expression: from west to east, these are (1) Gökçeyazı (GS) and (2) Kepsut (KS) fault segments (Figure 3).

The westernmost segment of the Havran-Balya Fault lies between Küçükdere and Hallaçlar and consists of many parallel/subparallel fault strands. From a map view,

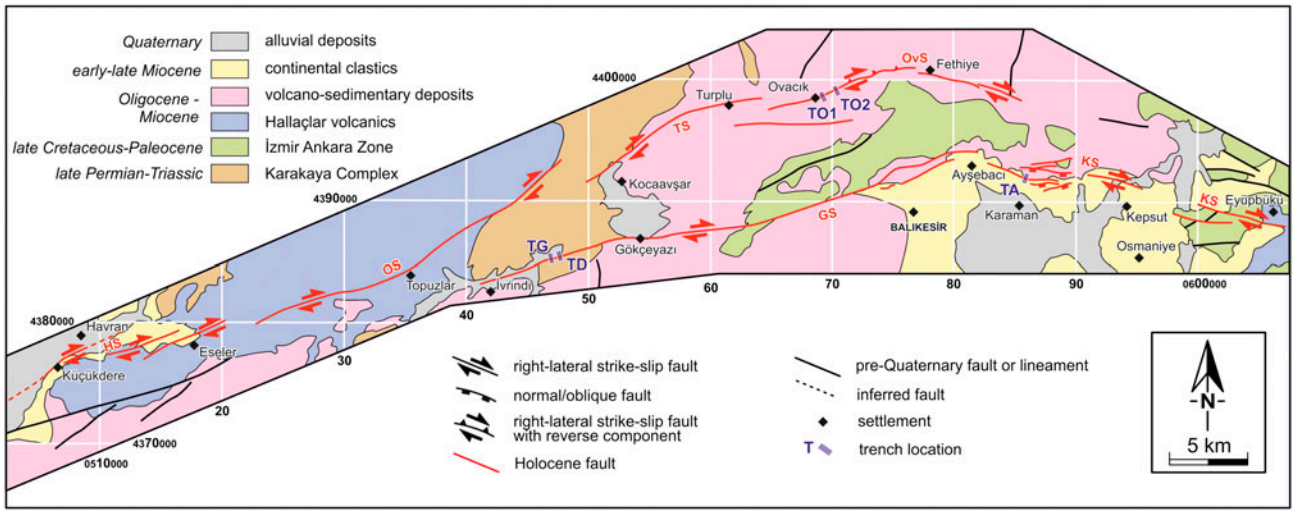


Figure 3. Simplified geological map showing fault segments of HBFZ and trench locations.
Source: Compiled from Duru, Pehlivan, Okay, Şentürk, and Kar (2012), Emre et al. (2011) and this study.
Abbreviations: HS, Havran Segment; OS, Osmanlar Segment; TS, Turplu Segment; OvS, Ovacık Segment; GS, Gökçeyazı Segment; KS, Kepsut Segment; TG, Güngörmez trench; TD, Dede trench; TO1, Ovacık-1 trench; TO2, Ovacık-2 trench; TA, Ayşebacı trench.

this segment has a clear right-stepping geometry along the southern rim of Edremit plain. The 13-km-long Havran fault segment represents the structural contact between the modern basin-fill of the Edremit plain and pre-Quaternary bedrock. Typical right-lateral offsets of the main streams where it crosses the fault trace suggest the dextral sense of movement along the Havran fault segment. The present morphology of the area between Eseler and Kocaavşar is shaped by the approximately ENE–WSW-striking and 25-km-long Osmanlar fault segment. It cuts the Oligo-Miocene volcanic rocks at the east of the Topuzlar town and juxtaposes them in northern block against the rocks of İzmir-Ankara Zone in the southern block (Figure 3). The NE–SW-trending Turplu fault segment is 15 km long and 1 km wide and has a s-shaped fault geometry lying between Kocaavşar and Turplu. North of Turplu, the segment direction turns to N80°E from N50°E with a spectacular bend. After that, the Turplu segment steps right at the west end of Turplu and passes to the Ovacık segment (Figure 3). This right-stepping jump also led to the formation of the Ovacık Quaternary pull-apart basin. The Ovacık segment represents the easternmost part of the Havran-Balya fault and extends about 22 km in the north of the Balıkesir city. It trends ENE–WSW for some distance around Ovacık, then bends into an approximately E–W direction around Fethiye, and finally bends toward the WNW–ESE direction in the east. This arched geometry of the Ovacık segment causes a transpressional area along the central part of the segment (Figure 3).

The Gökçeyazı fault segment that strikes N70–80°E between İvrindi and Ayşebacı extending over 40 km is the major structure of the HBFZ (Figure 3). It can be easily traced on topographic maps with various geomorphological features, such as aligned drainage systems, linear/sub-linear valleys, deflected stream channels, elongated hills and fresh fault scarps. The fault segment exhibits prominent Quaternary fault scarps and right-lateral displacements between Gökçeyazı and Balıkesir. The eastern part of the Gökçeyazı fault segment bounds the north side of the early-middle Miocene continental clastics and the southern side of the rocks of the İzmir-Ankara Zone. The easternmost part of the HBFZ is characterised by the Kepsut segment, which is a 25 km long, 1–3 km wide, N70°W-trending fault segment that includes at least 7 fault sets lying between Ayşebacı and Kepsut (Figure 3). Typically, each length of these faults can be traced up to a maximum of 10 km. The Kepsut segment cuts and displaces the Miocene volcano-sedimentary units and the rocks of İzmir–Ankara Zone, and laterally the offset is up to 300 m between Kepsut and Eyüpbükü.

Drainage systems are one of the significant lateral slip markers, because they continuously adapt their course to tectonic movement (Burbank & Anderson, 2001; Schumm, Dumont, & Holbrook, 2002). We measured the slip distributions on the segments of the HBFZ by field mapping geomorphic stream channel offsets. Offset amounts were determined using satellite images archived by Google Earth™, topographic maps of scale 1:25,000, and a digital elevation model based on these maps. Considering the initiation age of the NAF (beginning of the neotectonic period) in Marmara and that of the northern Aegean (Pliocene or late Pliocene) (Emre et al., 1998; Gürer et al., 2003; Okay, Demirbağ, Kurt, Okay, & Kuşcu, 1999; Okay et al., 2000; Ünay, Emre, Erkal, & Keçer, 2001), we can infer that the drainage network began to develop about 2.588 May ago.

Our observations along the HBFZ describe 11 right lateral cumulative displacements at 9 sites obtained from stream channels ranging from 125 to 9800 m (Figure 4 and Table 2). Larger offsets up to 9300 and 9800 m were

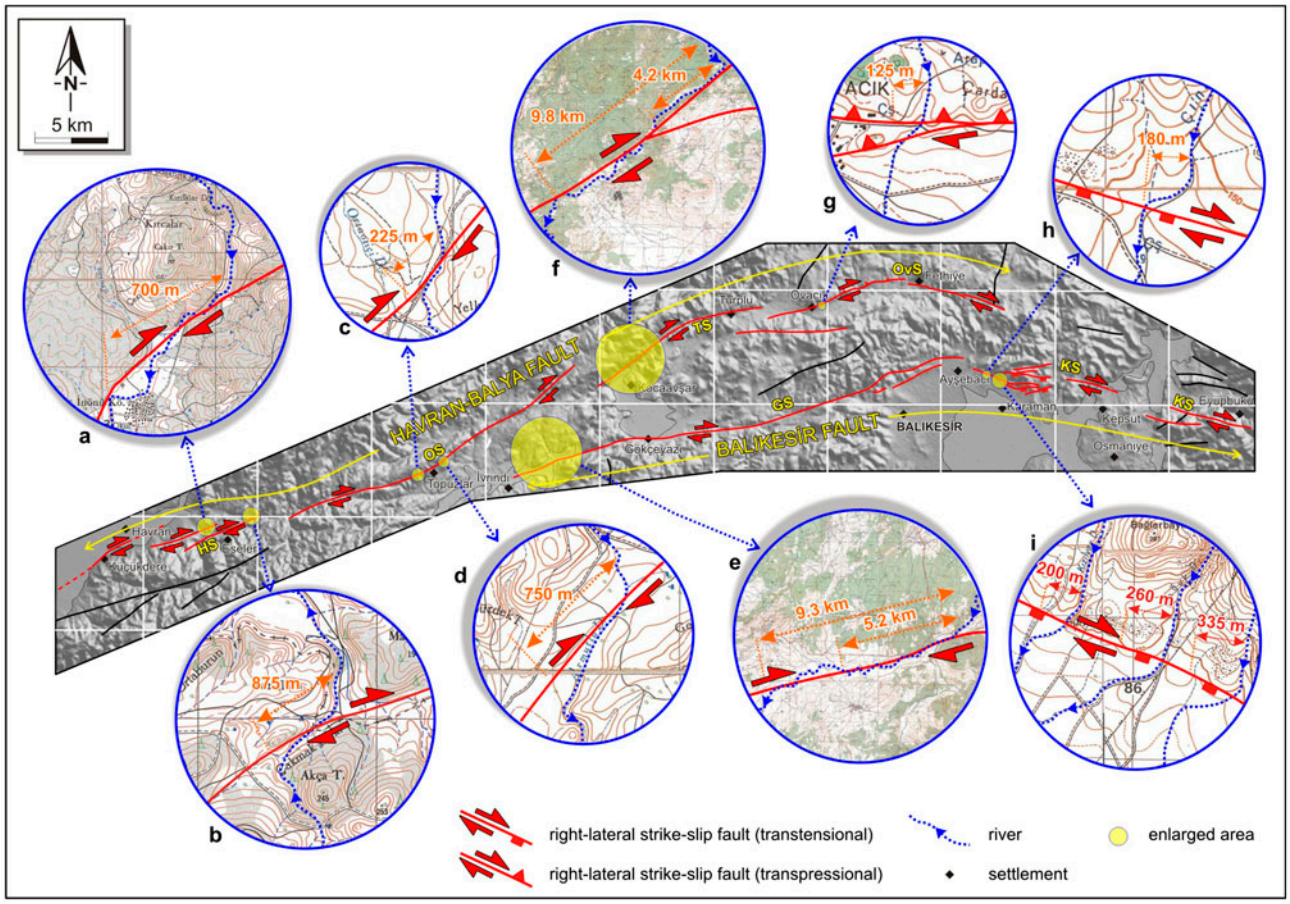


Figure 4. Morphotectonic map of HBFZ and measurement sites of offset streams.
Notes: See Figure 3 for map explanation. Table 2 provides detailed descriptions of offset stream channels.

Table 2. Description of offset stream channels along the HBFZ.

Site	Segment	Location	Coordinate long. (E)/lat. (N)	River	Displacment (m)
a	Havran	E of Havran	$^{05}13000$–$^{05}15000/^{43}82000$–$^{43}83000$	Badi	700
b		N of Eseler	$^{05}18000$–$^{05}19000/^{43}78000$–$^{43}80000$	Çakmak	875
c	Osmanlar	W of Topuzlar	$^{05}34000$–$^{05}35000/^{43}82000$–$^{43}83000$	Günbürdek	225
d		W of Osmanlar	$^{05}35000$–$^{05}36000/^{43}82000$–$^{43}84000$	Armutlu	750
e	Gökçeyazı	E of İvrindi	$^{05}37000$ –$^{05}46000/^{43}82000$–$^{43}85000$	Kocaçay	5200–9300
f	Turplu	N of Kocaavşar	$^{05}49000$–$^{05}58000/^{43}91000$–$^{43}99000$	Kocaçay	4200–9800
g	Ovacık	W of Ovacık	$^{05}68000$–$^{05}69000/^{43}98000$–$^{43}99000$	Arap	125
h	Kepsut	E of Ayşebacı	$^{05}84000$–$^{05}85000/^{43}92000$–$^{43}93000$	Çınarlı	180
i		N of Karaman	$^{05}85000$–$^{05}87000/^{43}91000$–$^{43}93000$	Kızılyar	200
				Koğuk	260
				Kazankaya	335

Note: For site locations see Figure 4.

measured from the central segments, yielding long-term slip rates of 3.59 and 3.78 mm/yr for Gökçeyazı and Turplu segments, respectively, while fewer values between 225 and 875 were observed along the western termination of the fault zone (Havran and Osmanlar segments). The smallest values ranging from 125 to 335 m on the Ovacık and Kepsut fault segments are directly associated with offsets dispersion on reversal and normal dip-slip components of the segment characteristics, respectively.

4. Palaeoseismology

In order to obtain detailed information on the frequency of surface faulting earthquakes, we excavated five palaeoseismological trenches on the HBFZ based on the

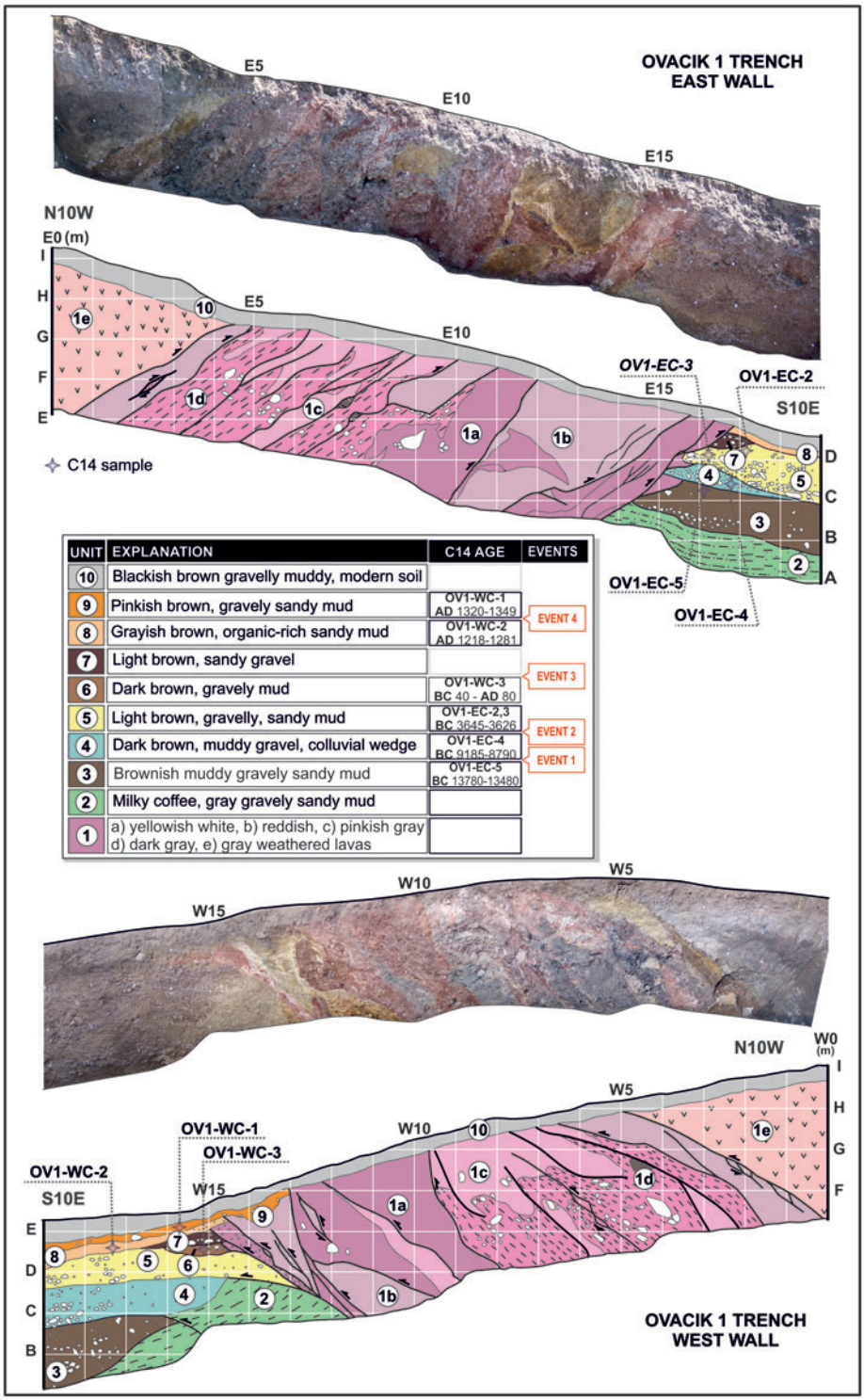


Figure 5. Field photographs and logged section of Ovacık-1 trench. (a) Oblique photomosaic and (b) logs of trench.
Note: See Figure 3 for trench location.

results of surface mapping. The microstratigraphy of the trenching area was determined by mapping the trench walls and C14 dating the lithostratigraphic units. Radiocarbon ages were calibrated to calendar years using the programme OxCal 4.2.4 (Bronk Ramsey, 2013) and based on atmospheric data from Reimer et al. (2013). Age ranges were rounded to the nearest 10 years. Dating analyses were carried out in the laboratories of Beta Analytic Inc. in Miami, Florida.

4.1. *Ovacık site trenches*

Two trenches (TO 1 and TO2) were excavated on the Ovacık fault segment.

Table 3. Radiocarbon age data from the HBFZ.

Trench name	Sample number	Lab. ID no	Material type	Radiocarbon age (BP)	Two sigma range (AD or BC)
Ayşebacı	AY-EC-2	392532	Organic sediment	1460 ± 30	550–648 AD
Ayşebacı	AY-EC-3	392533	Organic sediment	860 ± 30	1050–1080 AD
Ayşebacı	AY-EC-4	392534	Organic sediment	1280 ± 30	665–775 AD
Ayşebacı	AY-EC-5	392535	Organic sediment	470 ± 30	1415–1450 AD
Ovacık1	OV1-WC-1	392568	Organic sediment	540 ± 30	1320–1349 AD
Ovacık1	OV1-WC-2	392569	Organic sediment	770 ± 30	1218–1281 AD
Ovacık1	OV1-WC-3	392570	Organic sediment	1970 ± 30	40 BC–80 AD
Ovacık1	OV1-EC-2	392564	Organic sediment	4810 ± 30	3649–3626 BC
Ovacık1	OV1-EC-3	392565	Organic sediment	4800 ± 30	3645–3625 BC
Ovacık1	OV1-EC-4	392566	Organic sediment	9580 ± 40	9185–8790 BC
Ovacık1	OV1-EC-5	392567	Organic sediment	13020 ± 40	13780–13480 BC
Ovacık2	OV2-WC-1	392573	Organic sediment	780 ± 30	1215–1280 AD
Ovacık2	OV2-WC-2	392574	Organic sediment	710 ± 30	1265–1295 AD
Ovacık2	OV2-WC-3	392575	Organic sediment	1660 ± 30	335–425 AD
Ovacık2	OV2-WC-4	392576	Organic sediment	2940 ± 30	1226–1047 BC
Güngörmez	GUN-EC-1	392536	Charred material	3550 ± 30	1953–1870 BC
Güngörmez	GUN-EC-3	392538	Charred material	2980 ± 30	1280–1115 BC
Güngörmez	GUN-EC-5	392540	Organic sediment	2690 ± 30	900–800 BC
Güngörmez	GUN-EC-6	392541	Organic sediment	2730 ± 30	925–815 BC
Dede	DED-EC-1	392546	Organic sediment	6410 ± 30	5471–5319 BC
Dede	DED-EC-3	392548	Organic sediment	4720 ± 30	3630–3555 BC
Dede	DED-EC-4	392549	Organic sediment	5660 ± 30	4545–4450 BC
Dede	DED-EC-5	392550	Organic sediment	3570 ± 30	2015–1995 BC
Dede	DED-EC-6	392551	Organic sediment	7470 ± 30	6420–6250 BC

4.1.1. *Ovacık 1 (TO1)*

The Ovacık 1 trench is located at the eastern part of the Ovacık village (Figure 3). It is nearly 3.5 m wide, about 19 m long and 3.5 m deep. The trench wall shows the examples of transpressional deformations marked with prominent thrusting of Neogene basement over Quaternary clastic sediments (Figure 5). Basement rocks (unit 1) are represented by fractured and weathered volcanic rocks composed of dark grey, reddish brown and orangey yellow andesitic lavas. Holocene clastic sediments are colluviums that comprise angular and unsorted clasts in various sizes derived from the basement rocks. At the bottom, they start with the milky brown and greenish grey gravelly sandy mudstones of unit 2. The overlying unit (unit 3) is represented by brownish muddy gravel at the base, while the unit grades upward to a brown colour. In the Ovacık 1 trench walls, along the master fault where the fault planes separate volcanic bed-rock (unit 1) from the Holocene colluvium, three fault splays are logged. The undermost fault splay cuts unit 3 but is covered by unit 4. The triangular shape of unit 4 is interpreted as a colluvial wedge since it covers the fault tips and consists of a mixture of unsorted and angular gravel, sand and mud. Unit 4 is overlaid by unit 5, which consists of light brown gravelly and sandy mud. Dark brown gravelly mud (unit 6) and light brown sandy gravels (unit 7) are deposited in front of the uppermost fault splay. They are covered by greyish brown organic rich sediments of unit 8. Overlying unit 9 consists of pinkish brown gravelly sand mud. Finally, unit 10 is characterised by dark brown gravelly recent soil cover.

Based on the stratigraphical and sedimentological evidences and the analysis of structural elements, four past surface rupture events were identified in the Ovacık 1 trench. The earliest event occurred after deposition of the sediments of unit 3 and before deposition of the colluvial sediments of unit 4 (Figure 5). Hence, we collected samples from the upper part of unit 3 (sample OV1-EC-5) and the lower part of unit 4 (sample OV1-EC-4), which yielded calibrated ages between 13780–13480 BC and 9185–8790 BC, respectively (Table 2). These bracket the ages of the first event. The middle fault splay cuts unit 4 but is buried by the colluvial sediments of unit 5. While the lower boundary for the second event is limited by the age of unit 4 (sample OV1-EC-4) given above, the age of unit 5 represents the upper boundary. Samples OV1-EC-3 and OV1-EC-2 yielded a calibrated age between 3649 and 3625 BC, suggesting that the second event occurred before about 3637 ± 12 BC. The third event made a mark between unit 6 and unit 7 (Figure 5). The lower boundary for the third event is limited by the age of unit 6 (sample OV1-WC-3), which yielded a calibrated age of about 40 BC–80 AD, while the collected radiocarbon sample (OV1-WC-2) analysed from the sediments of unit 8 covering both unit 7 and also a third event gave a calibrated age of 1218 ± 52 AD. The uppermost fault splay cuts unit 8 and caused deposition of unit 9 (Figure 5). Hence, the youngest event took place between 1218 ± 52 AD and 1335 ± 15 AD (sample OV1-WC-1 analysed from the sediments of unit 9) (Table 3).

4.1.2. *Ovacık 2 (TO2)*

The Ovacık 2 trench is located about 1 km east of the Ovacık village (Figure 3). It is nearly 3.5 m wide, about

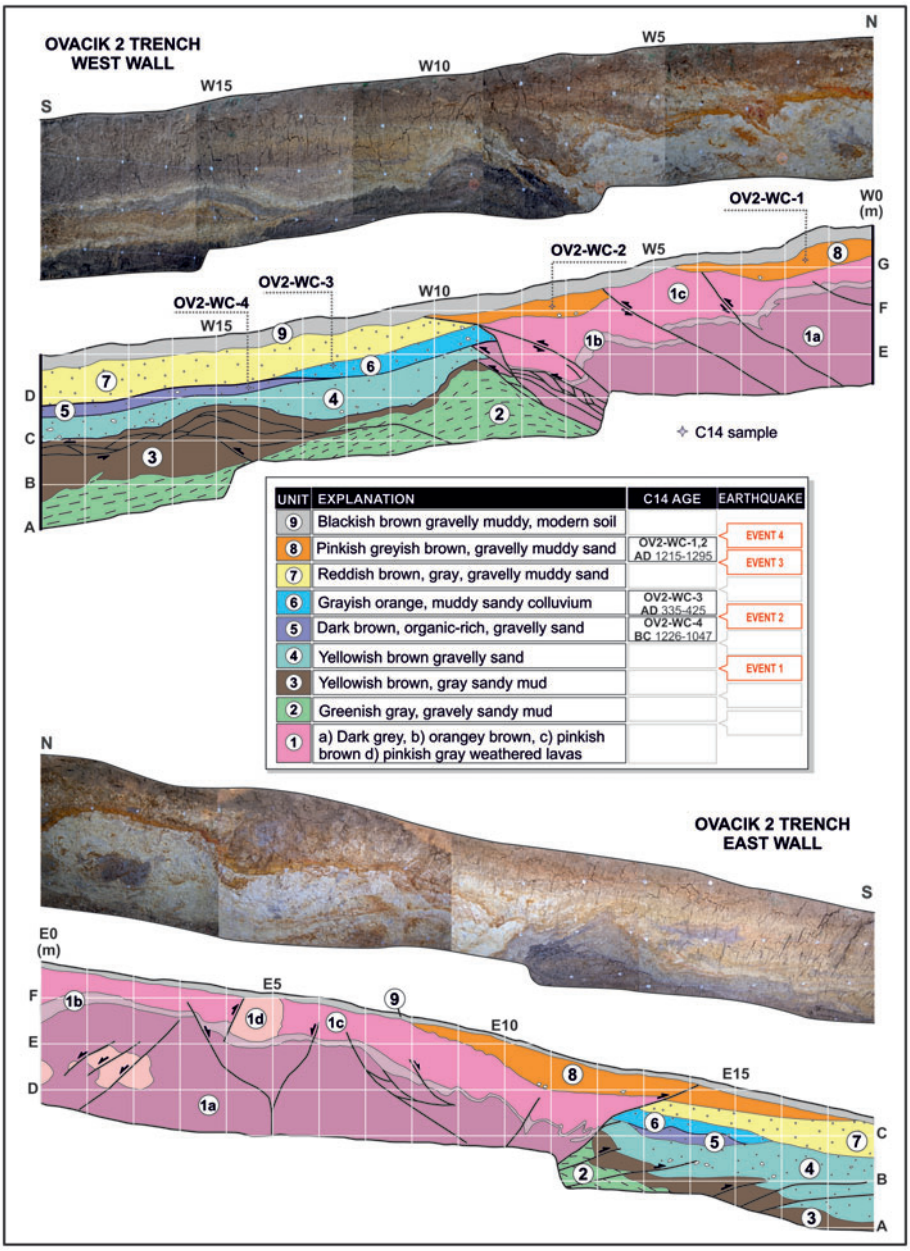


Figure 6. Field photographs and logged section of Ovacık-2 trench. (a) Oblique photomosaic and (b) logs of trench. Note: See Figure 3 for trench location.

19 m long and 3.5 m deep. The structural and stratigraphic setting of the Ovacık 2 trench wall is almost the same as the Ovacık 1 trench. Along the structural contact of the Neogene basement and the Quaternary sequence, three reverse fault splays are also exposed within the Ovacık 2 trench walls (Figure 6). The Neogene basement rocks (unit 1), which are shattered by many parallel/subparallel synthetic faults, are exposed in the uplifting hanging wall with in the trench. Unit 2 represents the bottom of the Holocene sequence in Ovacık 2 and comprise greenish grey gravelly sand and mud. The overlying unit 3 consists of yellowish brown sandy mud. These units are overlaid by the yellowish brown gravelly sand (unit 4) and brownish organic rich mud (unit 5) sediments. The overlying unit 6 consists of yellowish-greyish brown gravelly muddy sand, while unit 7 is composed of brownish organic rich gravelly mud. Dark brownish modern soil (unit 9) covers the unit 8 comprising pinkish brown gravelly, muddy sand (Figure 6).

Based on the stratigraphical and sedimentological evidences and the analysis of structural elements, four past surface rupture events were identified in the Ovacık 2 trench. Unit 4 covers the undermost fault splay, which is related with the first event. The radiocarbon age of unit 5 overlying unit 4 (OV2-WC-4) yielded a calibrated age between 1226 to 1047 BC, which provided the

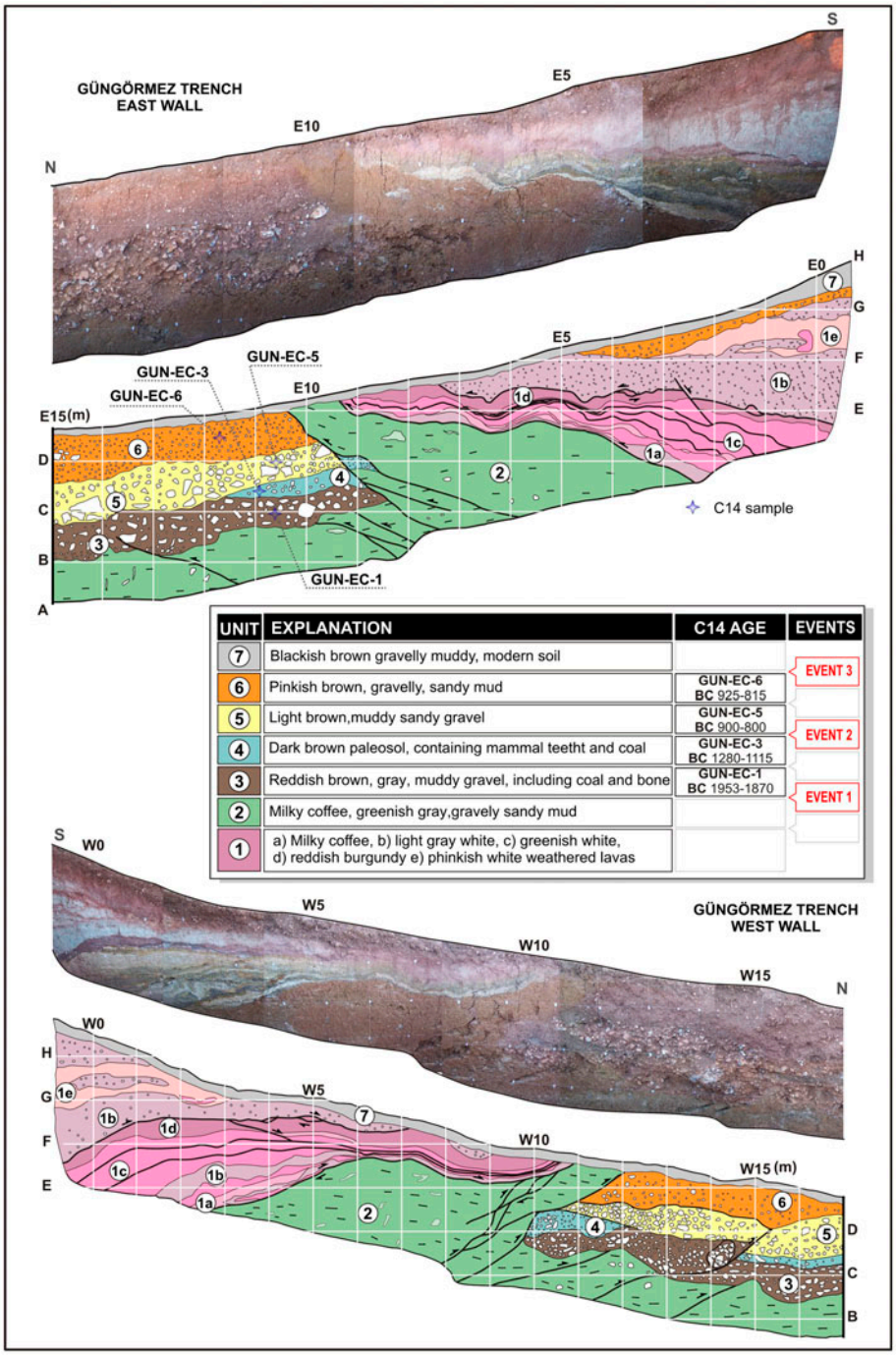


Figure 7. Field photographs and logged section of Güngörmez trench. (a) Oblique photomosaic and (b) logs of trench. Note: See Figure 3 for trench location.

upper boundary for the first event. Since the middle fault splay cut and deformed unit 4, the aforementioned calibrated age can be the lower boundary of the second event in the Ovacık 2 trench. Samples (OV2-WC-3) collected from the unit 6 exposed within the footwall yielded an age between 335 and 425 AD, which are the upper boundaries of the second event. The third event occurred before the deposition of unit 8 since unit 8 covers the fault, which is logged at the northern margin of the trench wall. Samples OV2-WC-1 and OV2-WC-2 were collected from unit 8 and yielded a calibrated age between about 1215–1280 and 1265–1295 AD, respectively, suggesting that the third event occurred before about 1248 ± 32 or 1280 ± 15 AD (Table 3). By the latest event, unit 8 is cut and displaced by both uppermost fault splay and backward synthetic fault. So, the latest event occurred after about 1248 ± 32 or 1280 ± 15 AD (Table 3 and Figure 6).

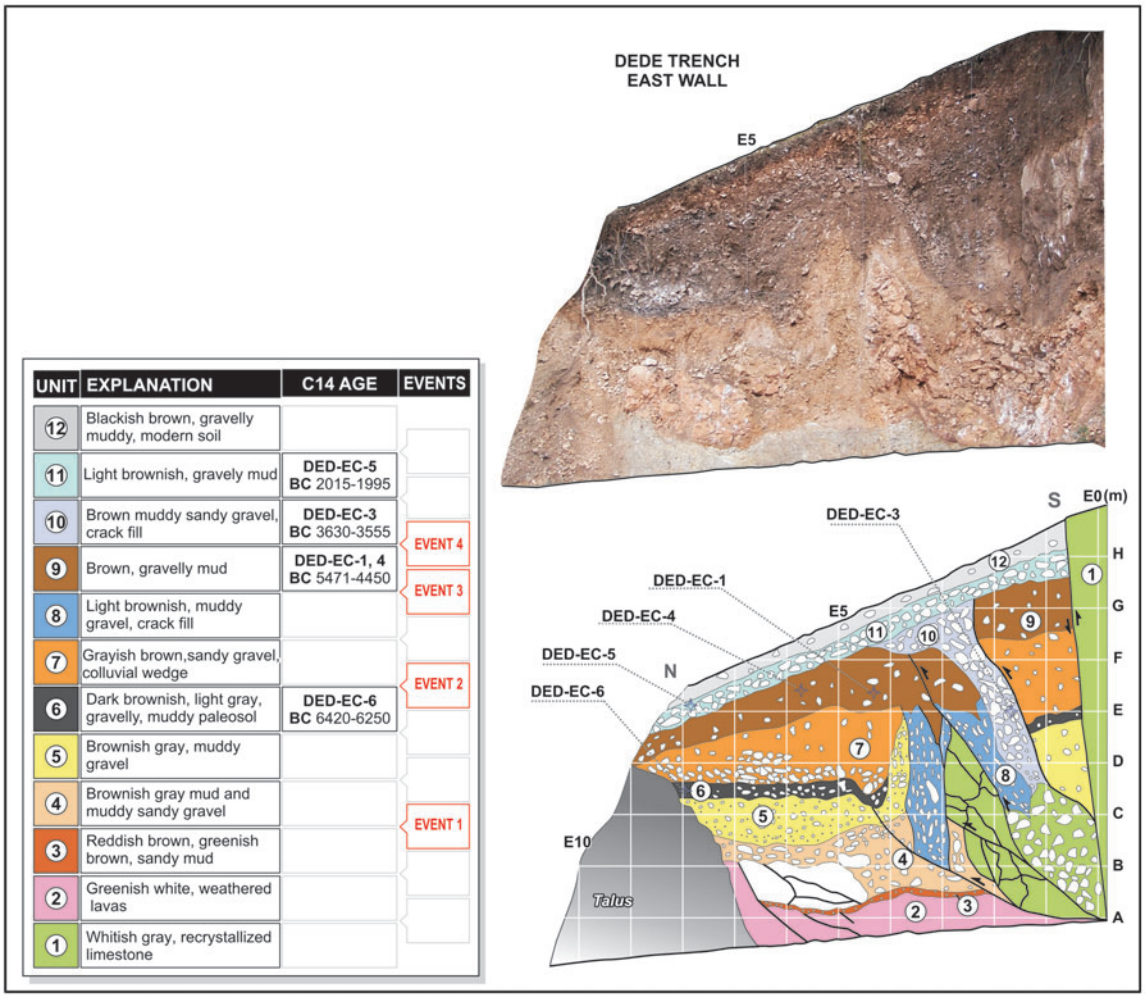


Figure 8. Field photographs and logged section of Dede trench. (a) Oblique photomosaic and (b) log of trench, eastern wall. Note: See Figure 3 for trench location.

4.2. *Gökçeyazı site trenches*

Two trenches (Dede and Güngörmez trenches) were excavated on the Gökçeyazı fault segment.

4.2.1. *Güngörmez trench (TG)*

Since the Gökçeyazı fault segment is cut and deformed upper Hollocene alluvial–colluvial deposits at the east of Gökçeyazı settlement where the fault scarps exhibits significant morphologic variations, this site was selected for palaeoseismic studies (for the trench location see, Figure 3). The Güngörmez trench is N–S oriented, nearly 3.5 m wide, about 15 m long and 3.5 m deep. On the uplifted hanging wall, the oldest unit (unit 1) consists of reddish claret-red, yellowish-greenish white and dark grey weathered volcanic rock. The Neogen basement rocks of unit 1 were thrust over unit 2 comprising milky brown gravelly sandy mudstone. Then, both of them started to push up and move to the higher strata over the Late Holocene alluvial/colluvial deposits by the reactivation of the Gökçeyazı fault segment. The bottom of the Late Holocene sequences overlies unit 2 with an angular unconformity and are composed of unsorted crudely stratified gravel and a cobble-pebble conglomerate (unit 3). Overlying unit 4 is represented by dark grey organic rich paleosol, including charcoal fragments, shells and mammalian teeth. Unit 5, comprising unsorted, subangular to subrounded clasts in sandy muddy infill, is overlaid by the deposits of brownish grey gravelly sandy mud (Unit 6) within the upper part of the trench walls. Unit 7 represents the present-day soil cover consisting of dark brown gravelly organic rich mud (Figure 7).

The Güngörmez trench provides direct stratigraphical evidence for at least three past earthquakes. Basinward synthetic fault splays within unit 2, possibly representing the same event, are covered by unit 3 in the northern side of the trench wall. Therefore, the radiocarbon sample GUN-EC-1, which was analysed from unit 3 and yielded calibrated ages between 1911 ± 41 BC, is the upper boundary for the oldest event. The lower limit of the first event yielded no result. The second event caused burial of the paleosol (unit 4). The sample GUN-EC-3

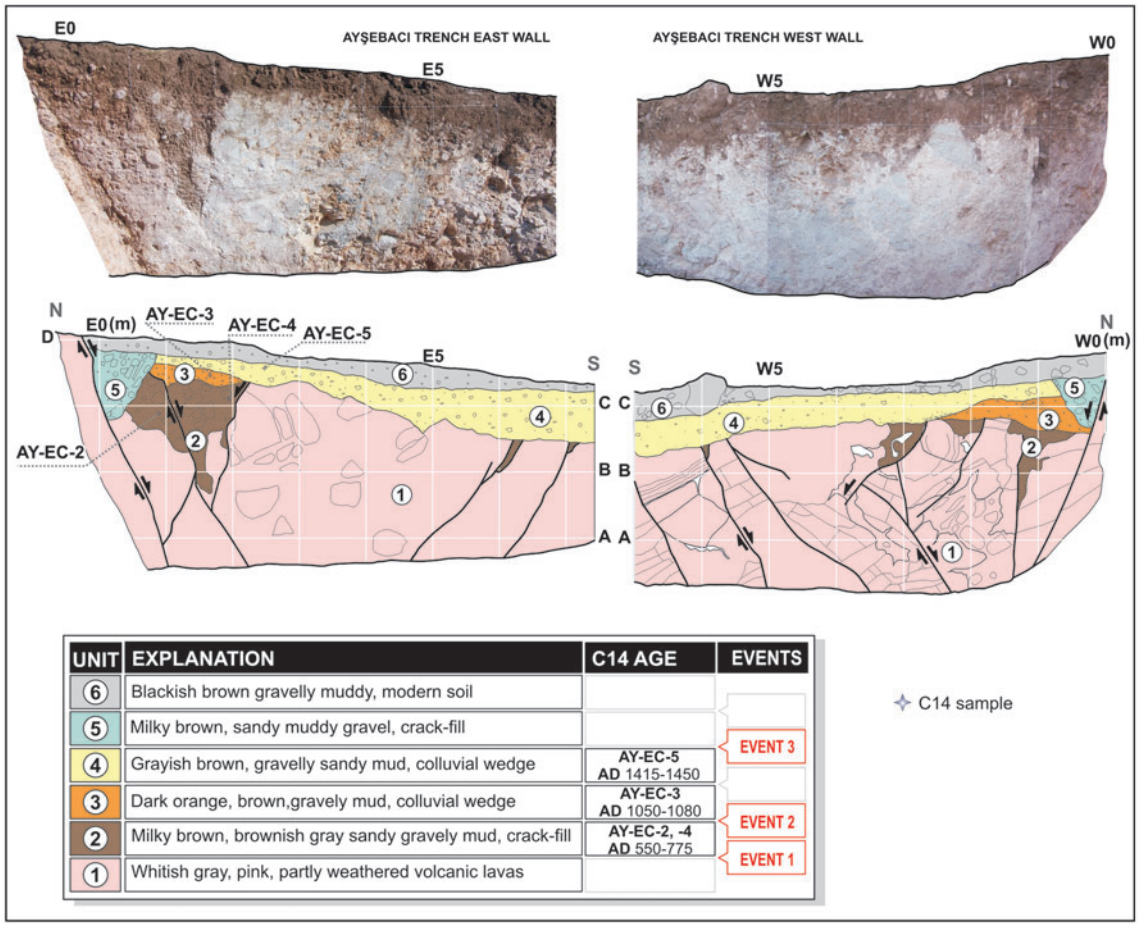


Figure 9. Field photographs and logged section of Ayşebacı trench. (a) Oblique photomosaic and (b) logs of trench.
Note: See Figure 3 for trench location.

analysed from unit 4 yielded a calibrated age of 1198 ± 83 BC and represents the lower boundary for the second event, while the upper boundary is represented by the radiocarbon age of sample GUN-EC-5 analysed from the unit 5, which yielded a calibrated age of 850 ± 50 BC (Table 3). The youngest fault splay cuts the all the units including units 5 and 6 except for the recent soil along the structural contact between uplifted unit 2 in hanging wall and late Holocene sequence in footwall. So the lower boundary of the youngest event is defined according to calibrated age of unit 6 (sample GUN-EC-6) which yielded calibrated age of 870 ± 55 BC. Thus, the youngest event took place sometime after 870 ± 55 BC (Table 3 and Figure 7).

4.2.2. *Dede trench (TD)*

Dede trench was excavated on the southern side of the Güngörmez trench where the colluvial deposits have contact with the master fault free surface in order to correlate them with the deposits in the Güngörmez trench (Figure 3). It is about 10 m long and 10 m deep, 15 m wide. Because of the presence of the unconsolidated loose and coarse grained colluvial deposit along the trench wall, it was hard to correlate the eastern and western wall. So, we studied mostly the eastern wall along which the structures could be observed better; only the eastern wall is presented here (Figure 8). Along the E–W-trending and south dipping Gökçeyazı master fault, basement rocks consisting of Mesozoic recrystallised limestones (unit 1) thrusted over the about 7-m high Holocene sequence consisting of fault-related clastics derived from the basement rocks and altered and deformed weathered volcanic rocks (unit 2). The Holocene sequence starts with reddish brown sandy mud (unit 3) and the brownish grey blocky gravelly mud and muddy sandy gravel alternation (unit 4). Overlying brownish grey muddy gravels (unit 5) are covered by organic rich dark brownish gravelly muds (unit 6). Unit 7 shows characteristics of colluvial wedge facies, including unsorted and angular greyish brown sandy gravels. Because of their geometry and nearly vertical clasts orientation with their long axis perpendicular to the surface, unit 8 is interpreted as the crack fills consisting of light brownish muddy gravels. Overlying unit 9 is composed of brown gravelly mud. After the deposition of units 9 and 10, comprising brown muddy blocky gravels, is deposited in a v-shaped crack opening, which deformed

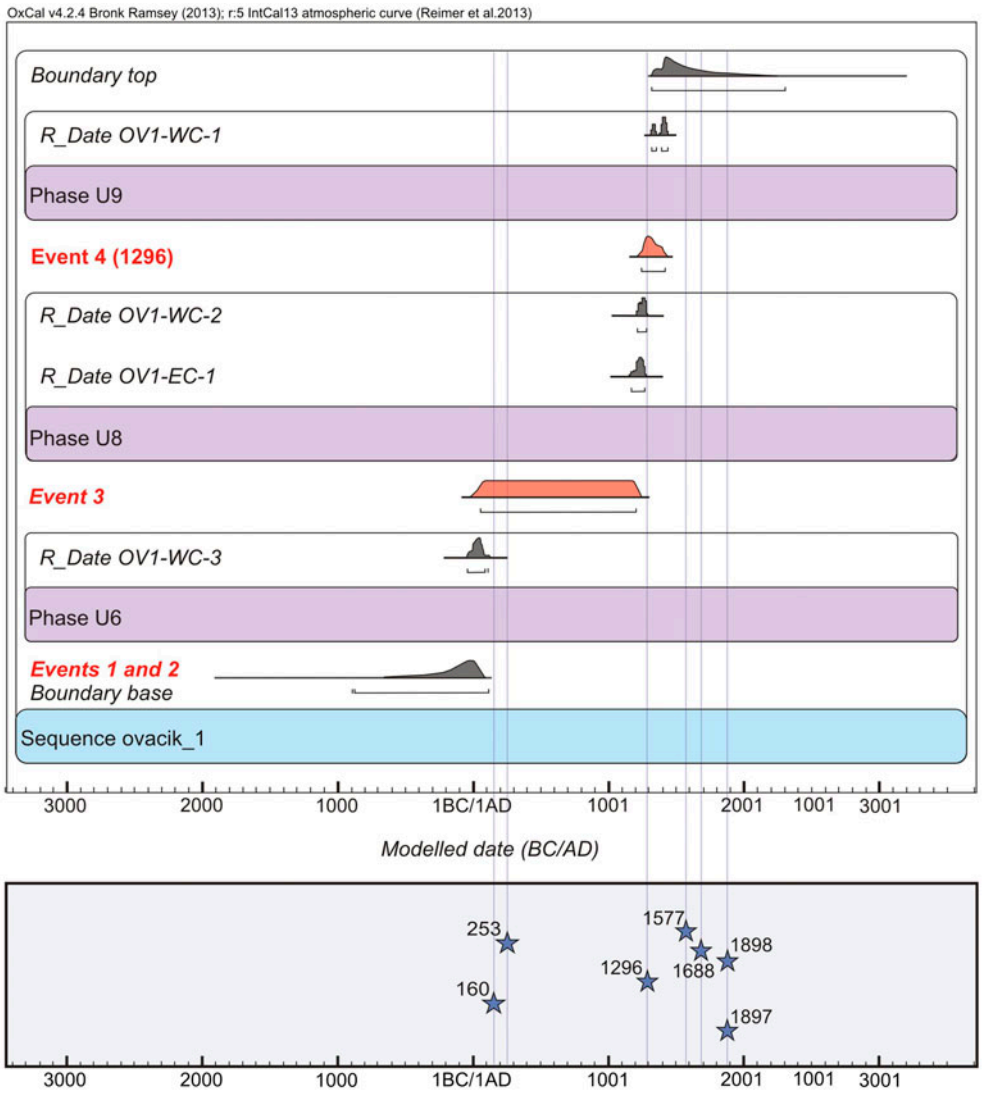


Figure 10. Probability distribution of calibrated ^{14}C ages obtained from sequential radiocarbon dates collected from the trench walls of Ovacık 1.

unit 9. Unit 10 is overlaid by 30 cm thick layers of unit 11, consisting of light brownish gravelly mud that is covered by the modern soil (unit 12) (Figure 8).

Based on the stratigraphical, sedimentological evidence and the analysis of structural elements, four past surface rupture events were identified in Dede trench. The first event took place before the deposition of colluvial sediments of unit 4. Unfortunately, we were unable to obtain the age of unit 4 because bulk samples do not have a sufficient amount of carbon for reliable dating. The second event occurred after the deposition of the paleosol (unit 6) and before the deposition of colluvial wedge (unit 7). The radiocarbon sample DED-EC-6, which was analysed from upper parts of unit 6 and yielded an origination date of 6335 ± 85 BC, is the lower boundary for the second event. The upper boundary for the second event is limited by the age of unit 9 (samples DED-EC-1 and DED-EC-4), which yielded origination between 5471 and 4450 BC (Table 3). The third event caused to crack fill, that is, to fill by the deposits of unit 8. So, the upper boundary of the third event is defined according to the calibrated age of overlying unit 9 (samples DED-EC-1 and DED-EC-4) given above, while the age of the unit 6 (sample DED-EC-6) represents the lower boundary, which dated to 6335 ± 85 BC. The latest event occurred before the deposition of crack fill sediments of unit 10. The uppermost levels of unit 9 (sample DED-EC-4) yielded 5660 ± 30 BP, suggesting the lower limit of the latest event. The age of the unit 10 (sample DED-EC-3), which yielded ages between 3630 and 3555 BC, is the upper limit of the latest event. The latest event is overlaid by 30 cm thick undeformed layers of unit 11 consisting of light brownish gravelly mud. The collected radiocarbon sample (sample DED-EC-5) analysed from the unit 11 gave a calibrated age between 2015 and 1995 BC, suggesting that no surface faulting earthquakes occurred after that time (Table 3 and Figure 8).

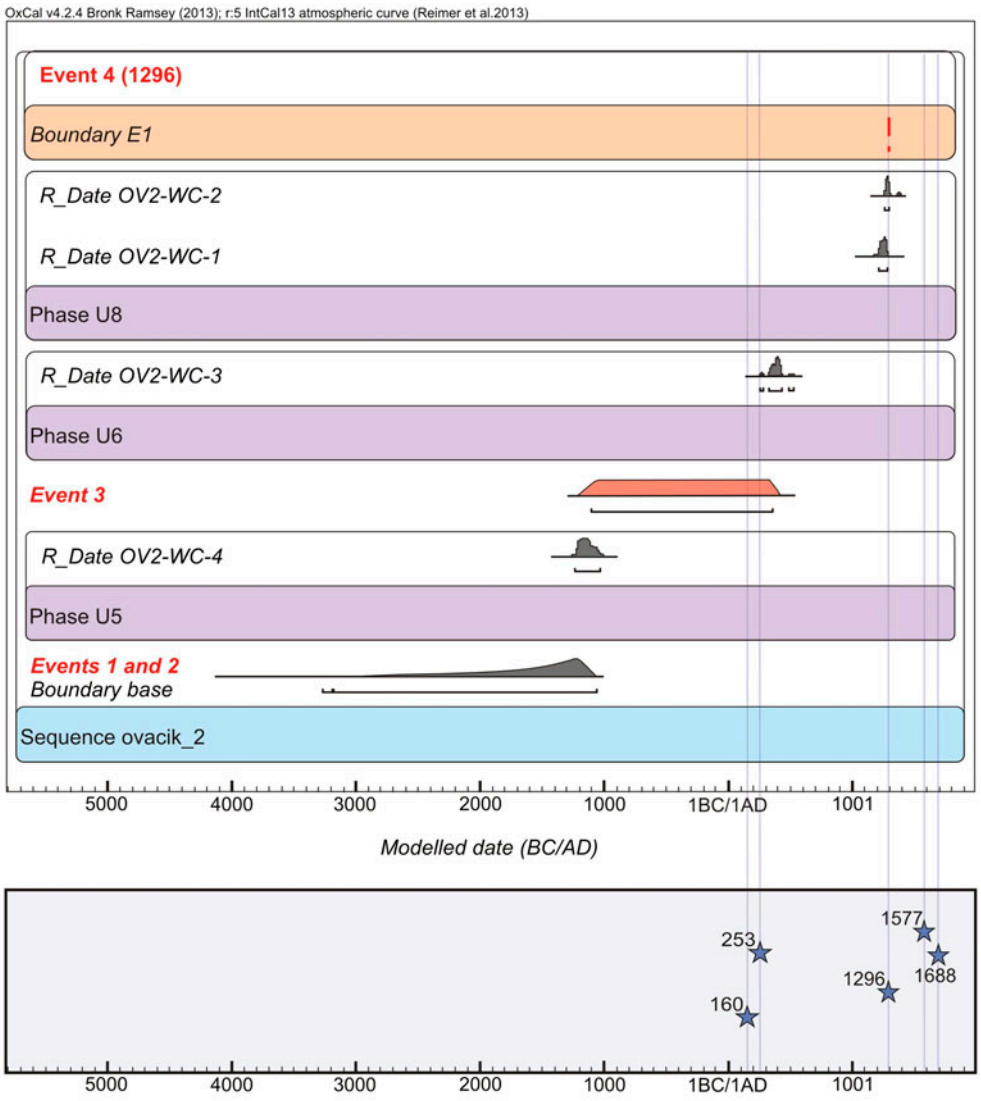


Figure 11. Probability distribution of calibrated ^{14}C ages obtained from sequential radiocarbon dates collected from the trench walls of Ovacık 2.

4.3. *Aysebacı Trench (TA)*

Aysebacı trench is located about 2 km north of the Karaman village (Figure 3) and was excavated at the site where the morphological expression of the Karaman fault scarp was best seen. It is N–S-oriented, roughly orthogonal to the local trend of the fault trace and is nearly 3.5 m wide, about 8 m long and 3.5 m deep. The trench walls clearly show six different units (Figure 9). Basement rock, which is cut and shattered by the Karaman fault, is represented by Miocene volcanic sequences consisting of whitish-grey, altered lava (unit 1). The rests are colluviums comprising of angular clasts in various sizes derived from the unit 1, except for unit 6, which is represented by organic rich modern soil sediments. Since both of its sides are bounded by the faults, its vertical v-shaped plan view and immature colluvial stratigraphy, it is likely that unit 2 is crack fills, including brownish-grey gravelly mud and light brownish sandy mud. Unit 2 is overlaid by unit 3 comprising dark brownish-orange, poorly consolidated and unsorted immature blocky organic rich gravelly mud. Colluvial sediments of unit 3 are overlaid by unit 4 comprising greyish brown gravelly sandy mud. Although its contact with the fault cannot be seen because of the interrupted crack fill during the latest event, it is likely that unit 4 is a remnant of colluvial because its sedimentologic significance indicating scarp-derived colluvium, its contents and grain sizes increasing towards to master fault, its v-shaped plan-view and its lower contact with an unconformity over the buried pre-faulting surface are prominent. Both units 4 and 3 are cut by unit 5, which is the uppermost v-shaped crack fill and is rich in bluish grey sandy and blocky gravel. A dark-reddish-brown organic soil horizon (unit 6) overlies the older units (Figure 9).

Based on the stratigraphical evidences and the analysis of structural elements, three events were identified in

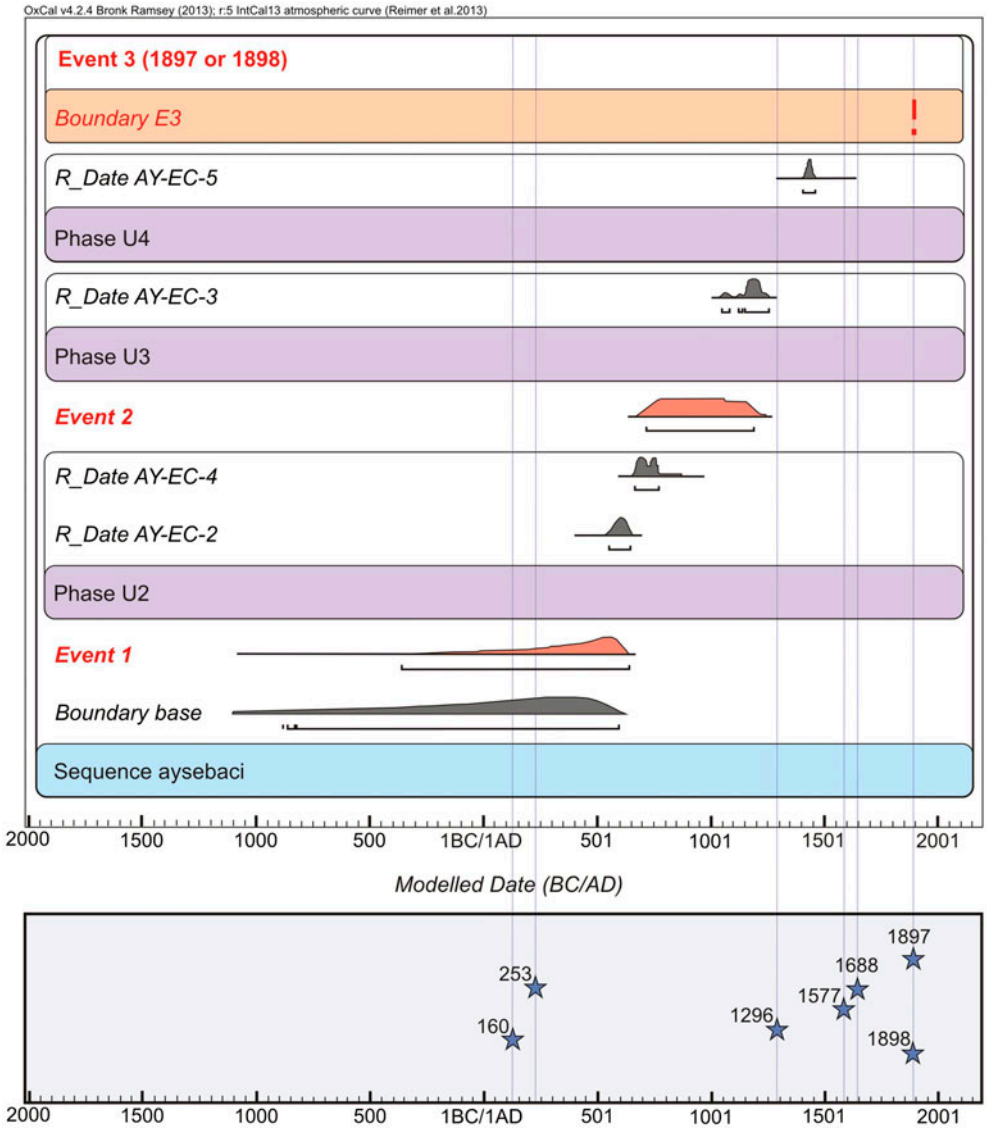


Figure 12. Probability distribution of calibrated ^{14}C ages obtained from sequential radiocarbon dates collected from the trench walls of Ayşebacı.

the Ayşebacı trench. The first crack fill (unit 2) is the product of the first event in the A1 trench. The radiocarbon samples AY-EC-2 and AY-EC-4, which were analysed from unit 2, yielded calibrated ages between 550–648 (599 ± 49) AD and 665–775 (720 ± 55) AD, respectively (Table 3). Aforementioned ages are the upper boundary for the first event and lower boundary for the second event because colluvial sediments of crack fill (unit 2) is cut and displaced by the synthetic faults during the Penultimate event. The vertical offset is about 57 cm. The collected radiocarbon sample (AY-EC-3) analysed from the colluvial wedge (unit 3) covering the second event gave a calibrated age between 1050and 1080 AD. Thus, the stratigraphic evidence and age results suggest that the second event occurred before 1065 ± 15 AD. The structural and stratigraphic evidences of the youngest surface rupture event exposed at the upper part in the northern part of the Ayşebacı trench. The crack fill identified as unit 5 cuts units 2, 3 and4. Since unit 4 is the youngest unit deformed by the youngest event, the calibrated age of the sample (AY-EC-5) analysed from unit 4 must represent the lower boundary of the latest event. These ages suggest that the youngest event took place after about 1432 ± 17 AD. (Table 3 and Figure 9).

5. Discussion and conclusions

The HBFZ is a 10–12 km wide, 100–120 km long, approximately N70°E-trending fault zone comprising several riedel faults that display a well-developed shear zone pattern with en échelon elongated hills. The fault zone comprised six main segments and displays morphological and kinematic evidences for dominantly dextral movement during the Holocene. According to structural and geomorphologic observations along the zone, the

fault segments have two different movement mechanisms. From west to east, the Havran, Osmanlar, Turplu, Ovacık and Gökçeyazı segments show strike-slip character, including a reverse component; on the other hand, the Kepsut segment representing the eastern most rim of the fault zone has dip/oblique-slip normal faulting character (Figure 3).

However, no large earthquake (M > 7) has occurred in the northern or central parts of the fault during the last 2000 years. We undertook a geomorphological and palaeoseismological investigation along the HBFZ with the aim of estimating the long-term slip rate and recurrence interval of strong earthquakes. Trenches were excavated at three sites. Detailed studies of trench cross-sections and dating (radiocarbon) show that HBFZ is responsible for some surface faulting earthquakes during the Holocene. The trenches excavated along the Ovacık Fault segment at the northern branch of HBFZ provide evidence for four events after 13630 ± 150 (Figures 10 and 11). Palaeoseismological evidence in the Ovacık site trenches suggests that the penultimate event took place sometime between 20 ± 60 AD and 1255 ± 40 AD, which can be correlated with the 160 or 253 earthquake considering historical records. The last event observed in both Ovacık 1 and 2 trenches on the Ovacık fault best fit with the 1296 AD earthquakes (Figures 10 and 11). So, the time after the last surface ruptured (M > 6) earthquake for the Ovacık fault segment is 719 years. Palaeoseismologic trench data yield a minimum recurrence interval of 1043 and a maximum recurrence interval of 1136 years for the Ovacık fault segment, which is about a 22 km-long active fault. Empirical relationships between the magnitude (Mb) and fault length show that the Ovacık fault segment is capable of generating an earthquake with a magnitude of 6.6 (Wells & Coppersmith, 1994).

Paleoseismic studies in Güngörmez and Dede trenches along the Gökçeyazı segment, the middle branch of HBFZ, indicate that the segment is responsible for some of the surface-faulting earthquakes before 0 AD. The Güngörmez trench suggests that the Gökçeyazı fault segment is active and caused three events; the first event occurred before 1911 ± 41 BC; the second one occurred between 1198 ± 83 BC and 850 ± 50 BC; and the latest event occurred sometime after 870 ± 55 BC. In the Güngörmez trench, the thickness of the unit 6 decreases or is missing at the hanging wall, and there are no fault scarps, topographically, between the dropped footwall and the uplifted hanging wall block. These factors indicate that the bottom horizon of the modern soil, especially along the uplifted hanging wall consisting of mostly basement rocks, is an erosional surface or is truncated by the basal surface of an agricultural layer, which cuts several ruptures including the master fault at the same stratigraphical horizon. Although the upper portion of the exposure at the hanging wall may not be complete, available data show that there is no evidence of surface rupture or associated ground deformation after 0 AD. in the trenches. Comparison of the estimated times of faulting yields a recurrence interval of 1000 years for the Gökçeyazı fault segment. According to the paleoseismic trench data and seismic records, the time after the last surface ruptured (M>6) earthquake for the Gökçeyazı fault segment is about 2000 years. Besides this, trench studies at the Gökçeyazı site indicate that the Dede trench includes older events than events in the Güngörmez trench. Field studies also show that the Gökçeyazı fault segment is about a 40 km-long active fault. Empirical relationships between Mb and fault length show that the Gökçeyazı fault segment is capable of generating an earthquake with a magnitude of 6.95 (Wells & Coppersmith, 1994).

Trench data from the Ayşebacı trench digging on the Kepsut Segment, at the eastern branch of the HBFZ, provide evidence for three events. The first of them occurred before 599 ± 49 AD and can be associated with 160 or 253 AD earthquakes, taking into account historical records (Figure 12). For the penultimate event observed in the trench, there is no record of any large earthquake in the Balıkesir area between 1065 ± 15 AD and 599 ± 49 AD. However, the latest event can be attributed to the 1897 event, which is the latest large earthquake record in the Balıkesir (Figure 12). According to the paleoseismic data along the Kepsut fault segment, an estimated recurrence interval of surface-ruptured earthquakes is about 1000 years. The time after the last surface ruptured (M > 6) earthquake for the Kepsut fault segment is 118 years. Field studies also show that the Kepsut fault segment is a 25 km-long south-facing active fault. Empirical relationships between Mb and fault length show that the Kepsut fault segment is capable of generating an earthquake with a magnitude of 6.7 (Wells & Coppersmith, 1994).

Consequently, geologic, geomorphologic and palaeoseismologic studies along the HBFZ indicate that the Kepsut, Gökçeyazı and Ovacık fault segments are capable of generating an earthquake with a moment magnitude of up to 7.2 and have an average recurrence interval of 1000–2000 years for surface-ruptured earthquakes. Recent palaeoseismologic studies carried out on the Gemlik and İznik-Mekece faults in the eastern part of the SMR indicates that the recurrence intervals of the southern branch of NAF are different than each other and changes between 595 and 1700–2200 years (Özalp et al., 2013; Yoshioka & Kuşcu, 1994). However, according to the palaeoseismologic studies in the central part of SMR performed along the YGF estimates the recurrence interval of 660 ± 160 years (Kürçer et al., 2008) and 420 ± 170 years (Belindir, 2008) for surface-faulting earthquakes. Our findings reveal that the earthquake recurrence interval of the segments of the HBFZ is not lower than 1000 years and irregular. Considering the fact that there was no evidence of a surface-ruptured earthquake for 2000 years, it can be stated that there is a seismic gap on the Gökçeyazı fault segment.

The strike-slip rate can be estimated according to the offset of river channels and their timing of formation

(e.g. Burbank & Anderson, 2001; Schumm, Dumont, & Holbrook, 2002). Mapping of fault traces along the HBFZ show that there are many regular single-stream offsets that reach 9.8 km. Based on the regional studies, we infer that the drainage system in SMR began to develop since the Pliocene or late Pliocene (Emre et al., 1998; Gürer et al., 2003; Okay et al., 1999, 2000; Ünay et al., 2001). We estimated the average slip rate of the HFBZ using the geomorphic markers such as river offset and the formation age of them. The Turplu and Gökçeyazı fault segments show a long-term right-lateral strike-slip rate of 3.59 and 3.78 mm/yr, respectively, from late Pliocene up to now. These values are lower than the slip rates inferred from the trenching on the Yenice-Gönen fault (11.66 mm/yr in Belindir [2008] and 6.3 mm/yr in Kürçer et al. [2008]) and short-term GPS data for SMR (5–7 mm/yr) (Armijo et al., 1999; Klinger et al., 2003; Meade et al., 2002). Hence, the HBFZ represents the southernmost border of the southern branch of the NAF, and the discrepancy of slip rates between previous studies performed in the centre or north of the SMR and this study indicates that the activity of the southern branch of the NAF decreases from north to south in the SMR.

Acknowledgements

We would like to gratefully and sincerely thank the Ovacık, Gökçeyazı, Kepsut and Karaman village headmen for their assistance and help during the excavation work. We would like to sincerely thank anonymous referees whose valuable comments and useful criticisms have greatly improved the manuscript. The paper was edited by American Manuscript Editors, an English language editing service.

Disclosure statement

No potential conflict of interest was reported by the authors.

Funding

This study is supported by National Earthquake Research Project No: UDAP-G-13-18 which has been realised in the frame of the Turkish Paleoseismological Project (TURKPAP).

ORCID

Hasan Sözbilir http://orcid.org/0000-0002-3777-4830
Çağlar Özkaymak http://orcid.org/0000-0002-0377-1324
Bora Uzel http://orcid.org/0000-0003-1703-5026
Ökmen Sümer http://orcid.org/0000-0003-3168-8728
Semih Eski http://orcid.org/0000-0002-2526-2571
Çiğdem Tepe http://orcid.org/0000-0002-2045-7310

References

Altınok, Y., Alpar, B., Yaltırak, C., Pınar, A., & Özer, N. (2012). The earthquakes and related tsunamis of October 6, 1944 and March 7, 1867; NE Aegean Sea. *Natural Hazards, 60*, 3–25.

Ambraseys, N. N. (1988). Engineering seismology. *Journal of Earthquake Engineering Structural Dynamics, 17*, 1–105.

Ambraseys, N. N. (2002). The seismic activity of the Marmara Sea region over the last 2000 years. *Bulletin of the Seismological Society of America, 92*, 1–18.

Ambraseys, N. N., & Finkel, C. F. (1995). *The seismicity of Turkey and adjacent areas: A historical review, 1500–1800*. İstanbul: Eren.

Ambraseys, N. N., & Jackson, J. A. (1998). Faulting associated with historical and recent earthquakes in the eastern Mediterranean region. *Geophysical Journal International, 133*, 390–406.

Armijo, R., Meyer, B., Hubert, A., & Barka, A. (1999). Westward propagation of the North Anatolian fault into the northern Aegean: Timing and kinematics. *Geology, 27*, 267–270.

Barka, A. (1992). The North Anatolian fault zone. *Annales Tectonicae, 6*, 164–195.

Barka, A. (1997). Neotectonics of the Marmara region in active tectonics of northwest Anatolia. In C. Schindler & M. Pfister (Eds.), *The Marmara poly-project* (pp. 55–87). Zürich: Hochschul-verlag AG an der ETH.

Belindir, F. (2008). *Neotectonic characteristics and paleoseismology of the Yenice-Gönen fault zone (NW Anatolia, Turkey)* (PhD thesis). Hacettepe Üniversity, The Graduate School of Natural and Applied Sciences, Ankara, 270 p.

Bozkurt, E. (2001). Neotectonics of Turkey: A synthesis. *Geodinamica Acta, 14*, 3–30.

Bronk Ramsey, C. (2013). OxCal 4.2. Retrieved from http://c14.arch.ox.ac.uk/oxcal

Burbank, D. W., & Anderson, R. S. (2001). *Tectonic geomorphology*. Malden, USA: Blackwell Science, 274 pp.

Duru, M., Pehlivan, Ş., Okay, A. İ., Şentürk, Y., & Kar, H. (2012). Biga Yarımadası'nın Tersiyer öncesi jeolojisi [Pre-Tertiary geology of Biga Peninsula]. In E. Yüzer & G. Tunay (Eds.), *Biga Yarımadası'nın Genel ve Ekonomik Jeolojisi* [General and Economic Geology of Biga Peninsula] *Special series, 28*, (pp. 7–74). Ankara, Turkish: MTA.

EMSC, Euro-Med Seismological Centre. Retrieved from http://www.emsc-csem.org

Emre, Ö., & Doğan, A. (2010). *1:250,000 scale active fault map series of Turkey, Ayvalık (NJ 35-2) quadrangle* (Serial Number: 4). Ankara-Turkey: General Directorate of Mineral Research and Exploration.

Emre, Ö., Doğan, A., & Özalp, S. (2011). *1:250,000 scale active fault map series of Turkey, Balıkesir (NJ 35-3) quadrangle. Serial number: 2*. Ankara-Turkey: General Directorate of Mineral Research and Exploration.

Emre, Ö., Doğan, A., & Yıldırım, C. (2012). Biga Yarımadası'nın diri fayları ve deprem potansiyeli [Active faults and earthquake potential of Biga Peninsula]. In E. Yüzer & G. Tunay (Eds.), *Biga Yarımadası'nın Genel ve Ekonomik Jeolojisi* [General and Economic Geology of Biga Peninsula] *Special series, 28*, (pp. 163–198). Ankara, Turkish: MTA.

Emre, Ö., Duman, T. Y., Özalp, S., Elmacı, H., Olgun, Ş. & Şaroğlu, F. (2013). *Açıklamalı Türkiye Diri Fay Haritası* [Annotated Active Fault Map of Turkey], *Special series, 30*, (pp. 89). Ankara, Turkish: MTA.

Emre, Ö., Erkal, T., Tchapalyga, A., Kazancı, N., Keçer, M., & Ünay, E. (1998). Neogene-quaternary evolution of the eastern Marmara-Black sea region, Northwest Turkey. *Bulletin of Mineral Research Exploration Turkey, 120*, 119–145.

Ergin, K., Güçlü, U., & Uz, Z. (1967). *A catalog of earthquakes for Turkey and surrounding area (11 A.D to 1964 A.D.),* (Report No. 24). İstanbul, Turkish: Istanbul Technical University Publications.

Gürer, Ö. F., Kaymakçı, N., Çakır, Ş., & Özburan, M. (2003). Neotectonics of the southeast Marmara region, NW Anatolia, Turkey. *Journal of Asian Earth Sciences, 21*, 1041–1051.

Herece, E. (1990). 1953 Yenice–Gönen deprem kırığı ve Kuzey Anadolu fay sisteminin Biga Yarımadası'ndaki uzantıları [1953 Yenice-Gönen earthquake rupture and extension of the North Anatolian fault system into the Biga Peninsula]. *General Directorate of Mineral Research and Exploration (MTA) Bulletin, 111*, 47–59.

Kalafat, D. (1998). Analyzed in terms of earthquake mechanisms of Anatolia tectonic structure. *Earthquake Research Bulletin, 77*, 1–217.

Kalafat, D., Kekovalı, K., Güneş, Y., Yılmazer, M., Kara, M., Deniz, P., & Berberoğlu, M. (2009). *A cataloque of source parameters of moderate and strong earthquakes for Turkey and its surrounding area (1938–2008)*. İstanbul: Boğaziçi University Publication 1026, pp. 1–43.

Kaymakcı, N. (2006). Kinematic development and paleostress analysis of the Denizli Basin (Western Turkey): Implications of spatial variation of relative paleostress magnitudes and orientations. *Journal of Asian Earth Sciences, 27*, 207–222.

Ketin, İ. (1957). Kuzey Anadolu Deprem Fayı [The North Anatolian Earthquake Fault]. *İstanbul Teknik Üniversitesi Dergisi, 15*, 49–52.

Ketin, İ. (1966). 6 Ekim 1964 Manyas depremi enasinda zeminde meydana gelen tansiyon çatlakları [Tension craks on the ground during the October 6, 1964 Manyas earthquake]. *Geological Bulletin of Turkey, 10*, 44–51.

Klinger, Y., Sieh, K., Altunel, E., Akoglu, A., Barka, A. A., Dawson, T., … Rockwell, T. (2003). Paleoseismic evidence of characteristic slip on the western segment of the North Anatolian fault, Turkey. *Bulletin of the Seismological Society of America, 93*, 2317–2332. doi:10.1785/0120010270

Kürçer, A., Chatzipetros, A., Tutkun, S. Z., Pavlides, S., Ateş, Ö., & Valkaniotis, V. (2008). The Yenice-Gönen active fault (NW Turkey): Active tectonics and palaeoseismology. *Tectonophysics, 453*, 263–275.

McClusky, S., Reilinger, R., Mahmoud, S., Ben Sari, D., & Tealeb, A. (2003). GPS constraints on Africa (Nubia) and Arabia plate motions. *Geophysical Journal International, 155*, 126–138.

McKenzie, D. P. (1972). Active tectonics of the Mediterranean region. *Geophysical Journal of the Royal Astronomical Society, 30*, 109–185.

Meade, B. J., Hager, B. H., McClusky, S. C., Reilinger, R. E., Ergintav, S., Lenk, O., … Özener, H. (2002). Estimates of seismic potential in the Marmararegion from block models of secular deformation constrained by GPS measurements. *Bulletin of the Seismological Society of America, 92*, 208–215.

Okay, A. İ., Demirbağ, E., Kurt, H., Okay, N., & Kuşcu, İ. (1999). An active, deep marine strike–slip basin along the North Anatolian fault in Turkey. *Tectonics, 18*, 129–147.

Okay, A. İ., Kaslılar-Özcan, A., İmren, C., Boztepe-Güney, A., Demirbağ, E., & Kuşcu, İ. (2000). Active faults and evolving strike–slip basins in the Marmara sea, Northwest Turkey: A multichannel seismic reflection study. *Tectonophysics, 321*, 189–218.

Özalp, S., Emre, Ö., & Doğan, A. (2013). The segment structure of southern branch of the North Anatolian fault and paleoseismological behaviour of the Gemlik Fault, NW Anatolia. *Bulletin of the Mineral Research and Exploration, 147*, 1–17.

Özkaymak, Ç. (2015). Tectonic analysis of the Honaz Fault (western Anatolia) using geomorphic indices and the regional implications. *Geodinamica Acta, 27*, 110–129. doi:10.1080/09853111.2014.957504

Özkaymak, Ç., & Sözbilir, H. (2012). Tectonic geomorphology of the Spildağı High Ranges, western Anatolia. *Geomorphology, 173–174*, 128–140.

Özkaymak, Ç., Sözbilir, H., & Uzel, B. (2013). Neogene-Quaternary evolution of the Manisa basin: Evidence for variation in the stress pattern of the İzmir-Balıkesir transfer zone, western Anatolia. *Journal of Geodynamics, 65*, 117–135.

Papazachos, B. C., & Papazachou, C. (2003). *The earthquakes of Greece*. Thessaloniki: Ziti publications, 286 pp (in Greek).

Reilinger, R., McClusky, S., Vernant, P., Lawrence, S., Ergintav, S., Cakmak, R., … Karam, G. (2006). GPS constraints on continental deformation in the Africa-Arabia-Eurasia continental collision zone and implications for the dynamics of plate interactions. *Journal of Geophysical Research, 111*, B05411.

Reimer, P. J., Bard, E., Bayliss, A., Beck, J. W., Blackwell, P. G., Bronk Ramsey, C., … van der Plicht, J. (2013). IntCal13 and Marine13 radiocarbon age calibration curves 0–50,000 years cal BP. *Radiocarbon, 55*, 1869–1887.

Rockwell, T., Barka, A., Dawson, T., Akyüz, S., & Thorup, K. (2001). Paleoseismology of the Gaziköy-Saros segment of the North Anatolia fault, northwestern Turkey: Comparison of the historical and paleoseismic records, implications of regional seismic hazard, and models of earthquake recurrence. *Journal of Seismology, 5*, 433–448.

Schumm, A. S., Dumont, J. F., & Holbrook, J. M. (2002). *Active tectonics and Alluvial rivers*. Cambridge: Cambridge University Press, 276 pp.

Shebalin, N. V., Karnik, V., & Hadzievski, D. (1974). *Catalogue of earthquakes*. Skojpe: UNESCO, 366 pp.

Soysal, H., Sipahioğlu, S., Kolçak, D., & Altınok, Y. (1981). *Historical earthquake catalogue of Turkey and surrounding area (2100 B.C. – 1900 A.D.)* (Report No. TBAG-341). Ankara: Tübitak Pub.

Sözbilir, H. (2001). Extensional tectonics and the geometry of related macroscopic structures: Field evidence from the Gediz detachment, western Turkey. *Turkish Journal of Earth Sciences, 10*, 51–67.

Sözbilir, H., Sarı, B., Uzel, B., Sümer, Ö., & Akkiraz, S. (2011). Tectonic implications of transtensional supradetachment basin development in an extension-parallel transfer zone: The Kocaçay Basin, western Anatolia, Turkey. *Basin Research, 23*, 423–448.

Stucchi, M., Rovida, A., Gomez Capera, A. A., Alexandre, P., Camelbeeck, T., Demircioğlu, M. B., … Giardini, D. (2013). The SHARE European earthquake catalogue (SHEEC) 1000–1899. *Journal of Seismology, 17*, 523–544.

Sümer, Ö., İnci, U., & Sözbilir, H. (2013). Tectonic evolution of the Söke Basin: Extension-dominated transtensional basin formation in western part of the Büyük Menderes Graben, western Anatolia, Turkey. *Jounal of Geodynamics, 65*, 148–175.

Şengör, A. M. C. (1979). The North Anatolian transform fault: Its age, offset and tectonic significance. *Geologial Society of London, 136*, 269–282.

Şengör, A. M. C., Görür, N., & Şaroğlu, F. (1985). Strike-slip faulting and related basin formation in zones tectonic escape: Turkey as a case study. In K. T. Biddle & N. Christie-Blick (Eds.), Strike-slip deformation, basin formation and sedimentation. *Special Publication – Society of Economic Paleontologists and Mineralogists, 37*, 227–264.

Şengör, A. M. C., & Barka, A. (1992). *Evolution of escape related strike-slip systems: Implications for distribution of collision orogens*. Abstracts, 29th IGC, Japan.

Şengör, A. M. C., Tüysüz, O., İmren, C., Sakınç, M., Eyidoğan, H., Görür, G., & Le Pcihon, X. (2005). The North Anatolian fault: A new look. *Annual Review of Earth and Planetary Sciences, 33*, 37–112.

Taymaz, T., Jackson, J., & Mc Kenzie, D. P. (1991). Active tectonics of the north and central Aegean Sea. *Geophysical Journal International, 106*, 433–490.

Tan, O., Tapırdamaz, M. C., & Yörük, A. (2008). The earthquake catalogues for Turkey. *Turkish Journal of Earth Sciences, 17*, 405–418.

Tan, O., & Taymaz, T. (2004). *Seismotectonics of the Caucasus and surrounding regions: source parameters and rupture histories of Recent destructive earthquakes,* AGU Fall Meeting, Session T53B, San Francisco-California, *EOS Transactions 85* (47), Abstracts T53B–0479.

Taymaz, T., Yılmaz, Y., & Dilek, Y. (2007). The geodynamics of the Aegean and Anatolia: Introduction. In T. Taymaz, Y. Yılmaz, & Y. Dilek (Eds.), *The geodynamics of the Aegean and Anatolia* (pp. 1–16). Special Publications 291. London: Geological Society.

Ünay, E., Emre, Ö., Erkal, T., & Keçer, M. (2001). The rodent fauna from the Adapazari pull-apart basin (NW Anatolia): Its bearings on the age of the North Anatolian fault. *Geodinamica Acta, 14*, 169–175.

Uzel, B., Sözbilir, H., Özkaymak, Ç., Kaymakcı, N., & Langereis, G. C. (2013). Structural evidence for strike-slip deformation in the İzmir-Balıkesir transfer zone and consequences for late Cenozoic evolution of western Anatolia (Turkey). *Journal of Geodynamics, 65*, 94–116.

Wells, D. L., & Coppersmith, K. J. (1994). New empirical relationship among magnitude, rupture length, rupture width, rupture area, and surface displacement. *Bulletin of the Seismological Society of America, 84*, 974–1002.

Yaltırak, C. (2006). Kazdağı'nın Tektonik Yapısı ve Edremit Körfezi'ni Karadan Sınırlayan Fayların Karakterleri [The tectonic structure of Kazdağı and character of faults which are bounding Edremit Bay from land]. *ATAG Bildiri Özleri Kitabı, 10*, 94–95.

Yoshioka, T., & Kuşcu, İ. (1994). Late Holocene Faulting events on the İznik-Mekece fault in the western part of the North Anatolian fault zone, Turkey. *Bulletin of the Geological Survey of Japan, 45*, 677–685.

Zimmermann, F. (1945). *6.10.1944 tarihinde vuku bulan Ayvacık-Ayvalık yersarsıntısı* [Ayvacık-Ayvalık Earthquake ocurred on October 6, 1944] (Report No. 025.343 Dab0) Ankara: Earthquake Research Centre Pub.